CHAPTER 4

Characterization of zebrafish Traf6 and Ikk2 mutants

4

Shuxin Yang[1], Natalia Nowik[1], Hongyuan Shen[3], Vladimir Korzh[3], Vinay Tergaonkar[3], Rubén Marín-Juez[2], Annemarie H. Meijer[1], Herman P. Spaink[1*]

1 Institute of Biology, Leiden University, P.O. Box 9502, 2300 RA Leiden, the Netherlands 2 Department of Developmental Genetics, Max Planck Institute for Heart and Lung Research, Ludwigstrasse 43, 61231 Bad Nauheim, Germany 3 Institute of Molecular and Cell Biology, Agency for Science, Technology and Research, Singapore, 138673 Singapore

Abstract

The Traf6 and Ikk2 proteins are partners in the signal transduction pathway underlying innate immunity and are involved in multiple pathological processes. Furthermore, they are also important for development, as shown by the fact that the total deficiency of Traf6 or Ikk2 in rodents is lethal. We analyzed zebrafish Traf6 and Ikk2 mutants with a stop codon in the reading frame of the protein coding sequences (*traf6*$^{sa244/sa244}$ and *ikk2*$^{m10/m10}$). We characterized the influences of these *traf6* and *ikk2* mutations on immunity and development. In the case of *ikk2* we also tested the response to hyperinsulinemia, since Ikk2 has previously been implicated in insulin signaling. Both mutants did not show any visible abnormal organ phenotype during embryonic or later developmental stages, and the adults were also capable of breeding. There were no consistent indications for effects on leukocyte phenotype in *traf6*$^{sa244/sa244}$. In contrast, *ikk2*$^{m10/m10}$ larvae showed a significant decrease in body size, leukocyte numbers and expression of marker genes for macrophages and neutrophils. For analysis of immune responses we infected the mutants with *Mycobacterium marinum* and measured bacterial proliferation. In the case of the *traf6* mutant no significant difference with the wildtype in susceptibility to infection could be observed and the surprising lack of phenotypes of this mutant is discussed. The *ikk2*$^{m10/m10}$ larvae showed a higher bacterial burden than *ikk2*$^{+/+}$ larvae upon *M. marinum* infection. In addition, in the *ikk2* mutant the insulin resistance induced by hyperinsulinemia was modulated. We also studied the inflammatory response induced by flagellin in the *ikk2* mutant through activating Tlr5 signaling. Unexpectedly, we found that in the *ikk2* mutant a significantly higher expression of *il1b* was induced than in the control. This result might be attributed to the overexpression of *ikk1* in the *ikk2* mutant, which perhaps plays a compensatory role in *il1b* expression induced by flagellin. Considering the phenotype of the *ikk2* mutant in both infection and insulin resistance this mutant provides new possibilities to further study the connection of innate immunity and metabolic diseases.

Introduction

Toll like receptors (TLRs) are an important class of pattern recognition receptors (PRRs). TLRs recognize conserved pathogen-associated molecular patterns (PAMPs) from microbial components and danger-associated molecular patterns (DAMPs) from the host itself. Thereby they initiate signaling pathways by the activation of NF-κB or AP-1 transcription factors and finally activate inflammatory and immune responses. Tumor necrosis factor receptor associated factor 6 (TRAF6), plays a critical role in mediating these processes. After signal transduction is initiated from the Toll/IL-1R (TIR) domain of TLRs, TRAF6 induces recruitment of MYD88 and IRAK1/4 to form a

receptor complex. Subsequently, TRAF6 dissociates from this receptor complex, and associates with TAK1, TAB1 and TAB2 to form a new complex. This new complex then translocates from the plasma membrane to the cytosol and is ubiquitinated by ubiquitin ligases UBC13 and UEV1A. Finally, it actives the MAPKs and the IKK complex (IKK1, IKK2 and NEMO), resulting in AP-1 and NF-κB activation (1, 2). In addition to functioning in the TLR/IL-1R signal transduction pathway, TRAF6 also interacts directly with TGFβRI/ALK5 (3, 4) and proteins from the TNF-receptor family, such as CD40 and TRANCER, also known as RANK (1, 5), that in turn activate the PI3K and downstream Akt/PKB pathway.

In mammals TRAF6 is broadly expressed in various tissues and cells, but most immune cells restrict their activity through selective expression of receptors used to activate TRAF6 (6). Moreover, TRAF6 has been shown to be critical for developmental processes (7, 8), bone metabolism (9) homeostasis (10), apoptosis (11) and cancer (12, 13). For instance, Traf6 knockout mice showed a high mortality within three weeks after birth, accompanied by severe defects in the encephalon and neural tube and abnormal regulation of the central nervous system (9, 14, 15). It has also been demonstrated that TRAF6 is important for the immune system, since Traf6-deficient chimeras generated a progressive lethal inflammatory disease associated with massive organ infiltration and a dominant Th2-type polarized autoimmune response (16). TRAF6 regulates the critical processes required for maturation, activation, and development of dendritic cells (DCs) (14). Mice that are deficient for Traf6 specifically in their regulatory T cells, developed allergic skin diseases, arthritis, lymphadenopathy and hyper IgE phenotypes (17). Furthermore, TRAF6 is a key component in the signaling cascade downstream of C-type lectin receptors and is a critical mediator of the anti-fungal immune response (18). TRAF6 is also required for production of IL-12 in control of parasite infections (19).

In the canonical NF-κB signaling, the IKK complex is activated by the TRAF6/TAK1/TAB1/ TAB2 complex. As the key catalytic subunit in the IKK complex, IKK2, also named as IKKβ or IKBKB, is essential for NF-κB activation in response to pro-inflammatory stimuli. Knockout of Ikk2 is lethal in mice (20, 21), but conditional knockout of Ikk2 can even reverse some pathological diseases and lesions induced by the IKK2/NF-κB signaling pathway. For instance, Ikk2 conditional knockout or inhibition in mice attenuates laser-induced choroidal neovascularization, a leading cause of blindness in the elderly (22), and reduces liver necrosis and inflammation from ischemia/reperfusion injury (23). However, mice with epidermis-specific deletion of Ikk2 develop a severe TNF-mediated inflammatory skin disease (24). Furthermore, Ikk2 has also been shown to be required for a proper response to infection in mice (25-28). For instance, previous studies indicate that selective ablation of lung epithelial Ikk2 impairs pulmonary Th17 responses and delays the clearance of Pneumocystis, an atypical fungal pathogen that causes severe, often fatal pneumonia in

immunocompromised patients (25). The pharmacological inhibition of IKK2 prevents human cytomegalovirus replication and virus-induced inflammatory response in infected endothelial cells (26). Interestingly, Ikk2 has also been implicated in insulin sensing, where heterozygous deletion of Ikk2 protected against the development of insulin resistance during high-fat feeding in obese ob/ob mutant mice (29). Moreover, inactivation of Ikk2 prevents insulin resistance in skeletal muscle by blocking fat-induced defects in insulin signaling (30).

Zebrafish has become an important vertebrate model for studying human diseases, such as cancer (31, 32), tuberculosis (33, 34), microbial infections (35, 36), neurodegeneration (37, 38), and developmental and metabolic diseases (39, 40). Their small size, transparent larvae and short generation time of 3-4 months are beneficial for the screening and imaging of transgenic lines. The excellent imaging tools and applicability of microinjection of disease inducing agents allow the study of the function of Traf6 and Ikk2 in different disease models in zebrafish. TRAF6 shows a highly conserved structure from mammals to zebrafish (5, 41, 42). In a previous study from our laboratory it was shown that Traf6 has a dynamic role as a positive and negative regulator in a zebrafish-Salmonella infection model, based on transcriptome profiling by a combination of microarray analysis and whole transcriptome deep sequencing of Traf6 morphants (43).

In this study, to further analyze the role of Traf6 and Ikk2 upon *Mycobacterium marinum* (Mm) infection, we conducted infection experiments using *traf6* and *ikk2* mutant zebrafish. We found that the *traf6* mutant display an absence of phenotypes that was not expected from results of previous studies. Specifically, we could not demonstrate an effect of the mutation in the defense of larvae to mycobacterial infection. Since we are not able to show any specific phenotype resulting from the mutation in Traf6 we consider it likely that it does not represent a null mutant, perhaps because of residual activity of a truncated protein or of the result of suppression by other mutations. In contrast, the *ikk2* mutant shows higher bacterial burden than wildtype upon infection with Mm. Furthermore, the *ikk2* mutant shows a reduction in the number of macrophages and neutrophils in the absence of infection. In addition, our studies revealed that *ikk2* mutation led to blocking of the insulin resistance induced by hyperinsulinemia. This indicates that the *ikk2* mutation might represent a null allele of this gene.

Results and discussions

Studies of a Traf6 mutant

1 Description of the traf6 mutation

The *traf6*^{sa244} mutant carries a guanine to thymine (G to T) point mutation that generates a premature stop codon located at the nineteenth amino acid close to the N-terminus of the RING domain (Fig. 1A). Theoretically, this leads in the homozygous situation to a complete absence of the Traf6 protein and prevents Traf6-mediated downstream signaling. To get rid of many of the background ENU mutations in the *traf6* mutant zebrafish, we conducted outcrosses between the wildtype and this mutant line (Fig. S1). The offspring from the fifth generation (F5) were used to conduct experiments in our study.

2 traf6 mutation affects the survival rate of zebrafish larvae

We performed an incross between the F0 generation of Traf6 heterozygotes, and only one male Traf6 homozygote offspring survived. This homozygote male was outcrossed to wildtype (AB/TL) to obtain the F2 generation of Traf6 heterozygotes (Fig. S1). Two groups of *traf6*$^{sa244/sa244}$, and *traf6*$^{+/+}$ larvae from the third generation (F3) (Fig. S1) were compared under normal embryo raising conditions to test for differences in unchallenged survival during development. Up to 7 dpf there was no difference in survival between mutants and wildtypes (Fig. 1B). After this period, *traf6*$^{sa244/sa244}$ larvae showed a significantly decreased survival rate (75% survival) compared with *traf6*$^{+/+}$ larvae (95% survival) (Fig. 1B). The steady mortality rates of *traf6*$^{sa244/sa244}$ larvae ceased at around 20 dpf. Thus, under our raising conditions, 8-20 dpf was a crucial period for raising *traf6*$^{sa244/sa244}$ larvae in this generation. Subsequent development of *traf6*$^{sa244/sa244}$ was normal with the larvae reaching adulthood in a normal time span leading to adults with a normal fertility rate at the expected time period. Furthermore, *traf6*$^{sa244/sa244}$ adults did not display any increased mortality rate compared with wildtype individuals and heterozygotes, or showing pathological features linked with infection.

In mice, Traf6 deficiency is known to influence bone development, for example Traf6-/- mice exhibit severe osteopetrosis and are defective in osteoclast formation (44) and Traf6 is involved in TNF-alpha-induced osteoclastogenesis (45). We therefore measured the body size of *traf6*$^{sa244/sa244}$ and *traf6*$^{+/+}$ zebrafish larvae at 5dpf (Fig. 1C). We found that there is no significant difference of the body size between *traf6*$^{sa244/sa244}$ and *traf6*$^{+/+}$ larvae.

3 traf6 mutation does not prevent activation of TLR signaling in zebrafish larvae

The premature stop codon in the mutant allele is predicted to lead to the disruption of almost the complete reading frame encoding the Traf6 protein. The resulting deficiency in the capacity of cells to induce the MYD88/IRAKs receptor complex and

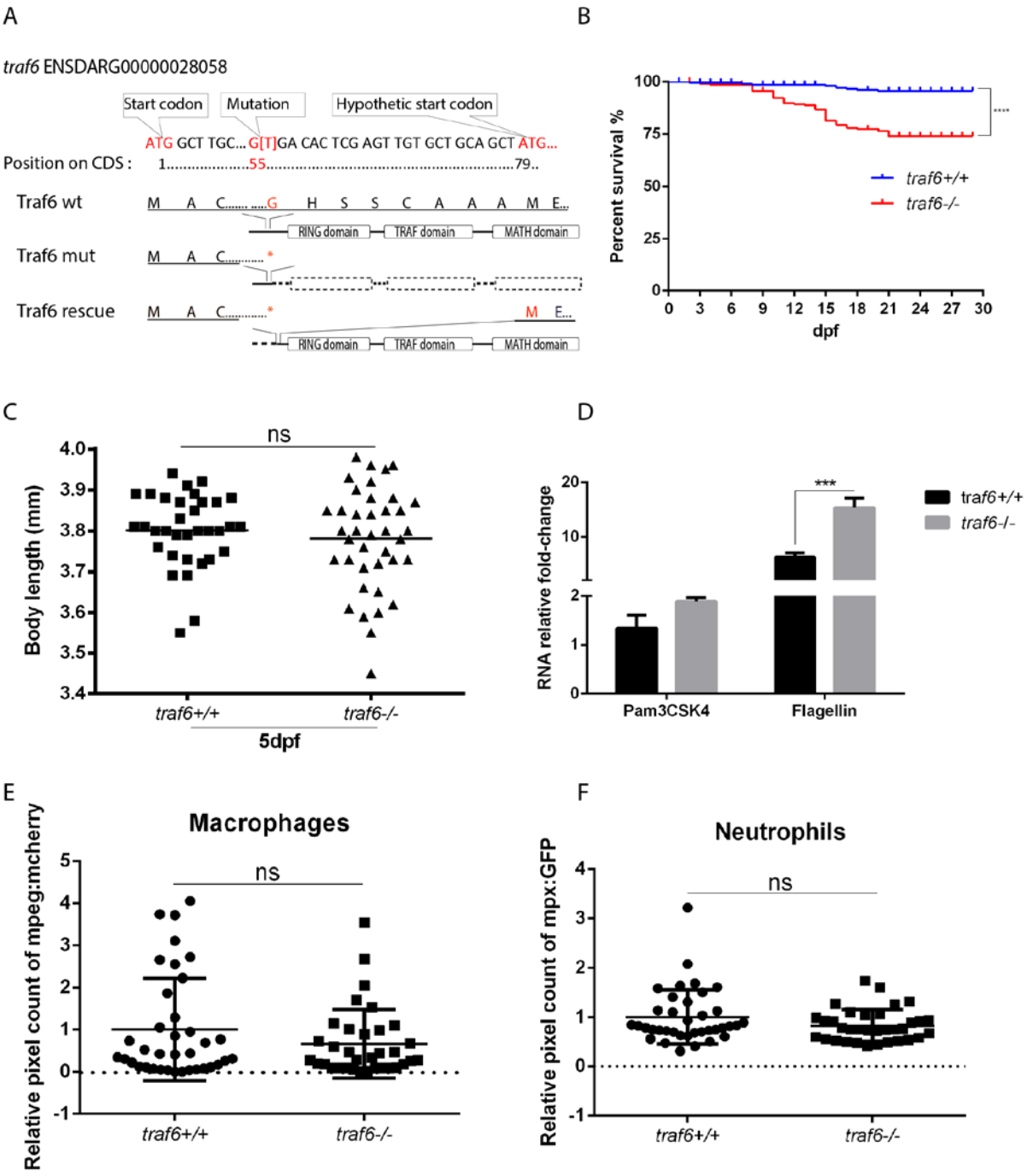

FIGURE 1 Description of the Traf6 mutant. A, mutant sequence and protein structure. A point mutation (G to T) in the codon for the nineteenth amino acid close to the N-terminus of the RING domain of zebrafish *traf6* introduces a premature stop codon. Nucleotide and amino acid positions are indicated with respect to the translation start codon. B, survival assays. Percentage survival during the first 20 days of development (under unchallenged conditions) is shown for two groups (n=70×3 per group) of *traf6*$^{sa244/sa244}$ mutants (red line) and *traf6*$^{+/+}$ wildtype (blue line), grown in three separate tanks. The groups are the F3 offspring of *traf6*$^{sa244/sa244}$ and *traf6*$^{+/+}$ siblings born from heterozygous parents. At 21 dpf, 95% of *traf6*$^{+/+}$ survived, 75% of *traf6*$^{sa244/sa244}$ mutants survived. The asterisks indicate the significant difference between wild-type and mutant survival (P<0.0001), tested

with a log rank test. C, body size measurement. Zebrafish larvae were imaged by stereo microscopy, and the body sizes were measured from *traf6*$^{+/+}$ and *traf6*$^{sa244/sa244}$ (n>30). D, *traf6*$^{sa244/sa244}$ and *traf6*$^{+/+}$ embryos were injected at 27 hpf with 1 ng Pam3CSK4 or 0.1 ng flagellin and expression levels of *il1b* were determined at 1hpi by qPCR. Data (mean ± SEM) are combined from at least three biological replicates (n=10 embryos per group) and expressed relative to their corresponding mock injection (water) control, which is set at 1. Statistical significance of differences was determined by two-way ANOVA with Sidak Multiple Comparison test as a post-hoc test, ***p<0,001. E-F, relative fluorescence pixel-count analysis of whole body number of mCherry-labeled macrophages and GFP-labeled neutrophils in 2dpf *traf6*$^{+/+}$*/Tg(mpeg1:mcherry/mpx:gfp)* and *traf6*$^{sa244/sa244}$*/Tg(mpeg1:mcherry/mpx:gfp)* embryos (n>30) were performed based on stereo fluorescence imaging. No significant differences were observed in both macrophages and neutrophils phenotype with a T-test.

activate TAK1/TABs, is expected to inhibit all TLR downstream signaling, including MAPK- and IKK complex-induced AP1 and NF-κB activation.

To confirm whether this *traf6* mutation blocks the downstream TLR signaling pathway, we analyzed the expression level of the inflammation marker gene *il1b* in zebrafish embryos upon injection with the TLR2 agonist Pam3CSK4 and the TLR5 agonist flagellin. Pam3CSK4 and flagellin were injected into the blood island of zebrafish embryos at 27 hpf. One hour post injection (hpi), we collected samples and conducted qPCR. We injected water (solvent for Pam3CSK4 and flagellin) as a control for which the gene expression level was set at 1 (Fig. 1D). In *traf6*$^{sa244/sa244}$ the expression level of *il1b* unexpectedly showed a significantly higher induction than that in *traf6*$^{+/+}$ upon flagellin injection, which remains unexplained (Fig. 1D). There was no significant difference of *il1b* expression between *traf6*$^{sa244/sa244}$ and *traf6*$^{+/+}$ upon Pam3CSK4 stimulation (Fig. 1D). These results show that the *traf6* mutation in our study does not block the TLR downstream signaling as we expected.

4 Macrophage and neutrophil phenotype in traf6 mutant larvae

GM-CSF and M-CSF promote macrophage proliferation, survival and differentiation through TRAF6-dependent AKT activation (46-50). A recent publication reported that the inhibition of TRAF6-mediated AKT activation is involved in macrophage proliferation regulated by CKIP (51), so our prediction is that a *traf6* mutation may influence the number of leukocytes in zebrafish. To study this we crossed *traf6*$^{sa244/sa244}$ into double transgenic *Tg(mpeg1.1:mCherryF/mpx:GFP)* fish, allowing the visualization of macrophages and neutrophils respectively. First, we analyzed leukocyte number by fluorescence pixel-count analysis of macrophages and neutrophils in 2dpf *traf6*$^{+/+}$*/Tg(mpeg1.1:mCherryF/mpx:GFP)* and *traf6*$^{sa244/sa244}$*/Tg(mpeg1.1:mCherryF/mpx:*

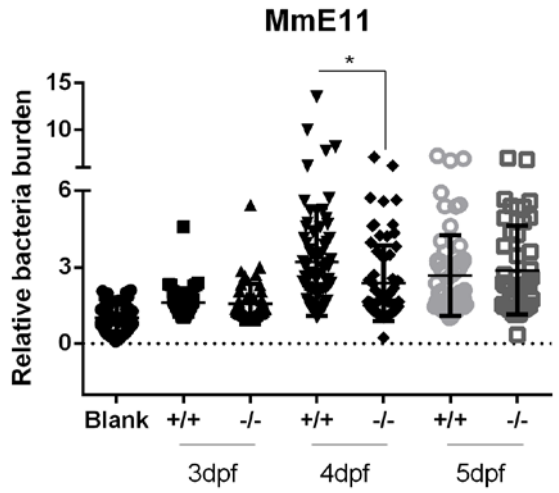

FIGURE 2 Quantification of bacterial burden in *traf6*$^{+/+}$ and *traf6*$^{sa244/sa244}$ larvae. Embryos were infected at 64-128 cell stage with ~40 CFU MmE11 strain. COPAS analysis were used for quantification of bacterial burden. Data (mean ± SD) are combined from two individual yolk infection assays . Statistical significance of differences was determined by one-way ANOVA with Tukey's Multiple Comparison method as a post-hoc test. *p<0,05, **p<0,01, ***p<0,001.

GFP) embryos. We observed no significant difference in the number of macrophages and neutrophils in the mutant (Fig. 1E-F).

5 Mycobacterium marinum infection in traf6 mutant larvae

We performed two individual yolk infection assays with *Mycobacterium marinum* E11 (MmE11) strain in the *traf6* mutant. We injected 64-128 cell stage embryos with ~40 cfu MmE11 by yolk injection, and conducted COPAS analysis at 3, 4 and 5 dpf (Fig. 2). The *traf6* mutant showed a decreased bacterial burden at 4dpf but not at 3 and 5 dpf (Fig. 2). Therefore we conclude that the *traf6*^{sa244}mutant allele does not have a major effect on host defense against Mm.

6 Western blot analysis of the Traf6 mutant

Considering the unexpected results of the phenotypic screening of the Traf6 mutant we tried to confirm that the mutation leads to a complete absence of Traf6 protein in zebrafish. Therefore we performed western blot analysis in 1dpf *traf6* morphants and 4dpf wt and mutant larvae (Fig. 3) using a commercially available monoclonal antibody against human TRAF6 protein. There was one band with a size close to the positive control TRAF6 protein from human Jurkat cells (58 kDa). The size of the predicted Traf6 protein in zebrafish is 62 kDa. The relative expression of this band that might represent zebrafish Traf6 was compared between different zebrafish samples using ImageJ analysis. The results showed that there was no significant difference of protein expression between wildtype and *traf6* morphants or *traf6* mutant larvae. One of the explanations for this result is that this protein band is not representing the Traf6

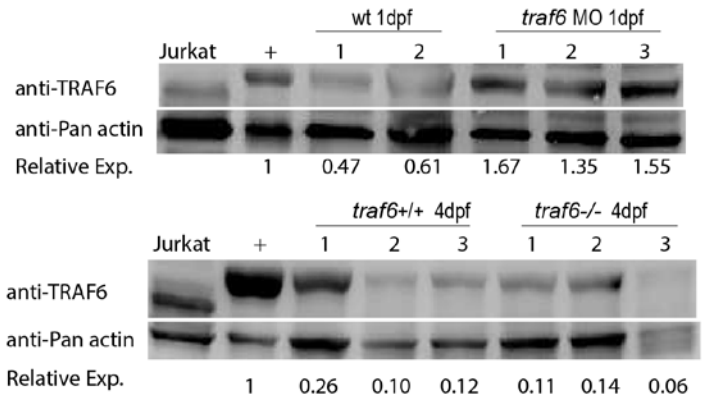

FIGURE 3 Western blot analysis of Traf6. Western blot results of whole 1 dpf embryos (*traf6* morphants and wildtype, upper two-panels) and 4 dpf larvae (*traf6* mutant and wildtype, lower two-panels) are shown. Relative expression data (mean ± S.E.M.) are determined from two (wt) or three (*traf6* MO, *traf6*+/+, *traf6*-/-) biological replicates (n=100 embryos (1dpf)/group (upper panel), n=15 larvae (4dpf)/group (lower panel)) and expressed relative to the positive control (+, whole protein from 4dpf AB/TL wildtype fish line), which is defined as 1. A protein sample of human Jurkat cells is included as a control for the antibody specificity. MO, morphants; wt, wildtype.

protein and that the antibody was not able to detect zebrafish Traf6 due to an aspecific background band. This is argued by the absence of an effect in the samples from treatment with a Traf6 translation blocking morpholino, which was previously shown to affect embryo development as well as the expression of immune effector genes downstream of Traf6 signaling (43). The other explanation is that the *traf6* mutation does not result in a null mutant at the protein level and that the *traf6* morpholino treatment isnot sufficiently penetrant to show an effect at the protein level.

7 Conclusion

In conclusion we can propose two possible explanations for the shown results.

Firstly, the point mutation from G to T at position 55 bp after the predicted start codon of Traf6 does not lead to a null phenotype *traf6* mutant. We hypothesize that there could be an alternative start codon close to the mutation point that leads to reinitiation of translation of Traf6. We did find that there is another ATG at the position 79 bp in the coding sequence (Fig. 1A) that if used as an alternative start codon would lead to a slightly shorter Traf6 protein. Although various of the amino acids in the resulting deletion are conserved in the mammalian counterparts, the entire RING domain would not be affected and therefore it is conceivable that the resulting protein might be at least partially or perhaps fully functional. However, we do not know how likely this hypothesis is, since to our knowledge the capacity of the zebrafish translation machinery to restart translation shortly after a stop codon that pertubs a natural reading frame is currently unclear.

Secondly, another explanation is that the *traf6* mutation effect has been rescued by another mutation in the genome that resulted from the saturating ENU methodology used for mutagenesis that was not bred out of the original founder line. An indication for this is that we only obtained one single homozygote after the first generation incross. Such a suppressor mutation could have led to misregulation of homologs of Traf6 that might take over the function of Traf6. It is also possible that the Traf6 mutation is suppressed by mutation of unrelated proteins that function in the TLR or TNF signaling pathways. This would be similar to the published suppression of mutants of Ikk2 by mutations in Tnfr1 (52). Li et al (52) showed that mice double mutants of $Tnfr1^{-/-}/Ikk2^{-/-}$ can survive until one month rather than die around 12.5-13.5 days like the $Ikk2^{-/-}$ mutant. They demonstrated that the rescue of embryonic lethality of Ikk2 deficiency by inactivation of Tnfr1 is caused by the inhibition of Tnfa-induced hepatocyte apoptosis. If Traf6 protein indeed is essential for development in zebrafish (as suggested by our previous morpholino results (43)) it is very much possible that we have selected for suppressor mutations during our incrossing schemes. An indication for this is the higher levels of lethality of larvae resulting from incrosses at the third generation after 7 days of development post fertilization (Fig.1B). For instance, it is possible that the larvae that died represent a population in which the suppressor mutation was lost or that the surviving population have optimized the effect of the suppressor mutation via epigenetic regulatory mechanisms.

In order to resolve these questions and to proceed with further studies of Traf6 in zebrafish it is needed to construct new mutants for comparative studies. Fortunately, during the time that this study was performed the new CRISPR/CAS technology has been made suitable for the efficient generation of targeted mutations also in zebrafish (53, 54). However, this study also illustrates that a limiting factor in zebrafish mutant studies is the lack of reliable antibodies against the studied signaling proteins. The availability of good antibodies against zebrafish Traf6 protein will remain extremely important for future studies of the function of this protein using new mutant lines.

Studies of an Ikk2 mutant

1 General characterization of ikk2 expression and ikk2 mutant zebrafish embryos

To show the transcription expression pattern of *ikk2* in zebrafish embryos, we collected RNA from wildtype (AB/TL) embryos to perform a time course qPCR series at different stages, which included oblong (3.7 hpf), germ ring (5.7 hpf), bud (10 hpf), 20-somite (19 hpf), 24 hpf, 48 hpf, 60 hpf and 72 hpf (Fig.4A). We found that the expression level of *ikk2* starts to show a stabilized expression from the 20-somite stage (19 hpf) until the last time point (72 hpf) of the assay (Fig.4A).

An *ikk2*^{m10} mutant was obtained from Dr. Vladimir Korzh's lab. These researchers developed this mutant by zinc finger nuclease-mediated mutagenesis. The *ikk2*^{m10} mutant carries an insertion mutation from AC to ATGC that creates a premature stop codon (Fig. 4B). The position of this stop codon located in the N-terminus of the kinase domain of zebrafish Ikk2 leads to a gene reading frame shift at the codon of the tenth amino acid and introduces a premature stop codon at the predicted sixty first amino acid. Technically, this should lead to a complete absence of the Ikk2 protein and prevent downstream signaling. Korzh et al. found that homozygote mutants carrying this predicted null allele showed survival rates comparable to wildtype from the one-cell stage until three months post fertilization, but decreased body lengths at nine months of age (unpublished data).This is in agreement with a previous study that shows that endothelial-specific Ikk2 knockout mice were ~25% smaller than the control (55). We measured the body length of zebrafish *ikk2* mutants at 3dpf, and found that, compared to their siblings control *ikk2*$^{+/+}$, *ikk2*$^{m10/m10}$ showed a significant shorter body length (Fig. 4C). This result is therefore in good agreement with the earlier unpublished studies of Khorz et al. and shows that this phenotype is already detectable at a very early stage of development.

To determine the RNA expression pattern of *ikk2* in the *ikk2* mutant, total RNA was isolated from embryos and qPCR was performed at 20-, 33-, 48- and 72 hpf. We found that the *ikk2* mutant showed a significant upregulation of the *ikk2* mRNA level at 3dpf (Fig. 4D). This suggests that the *ikk2* mutant induces an overexpression of *ikk2* at the transcriptional level in zebrafish early stage development or that the *ikk2*^{m10} mRNA is more stable than the wild type *ikk2* mRNA. This may indicate a negative feedback regulation of Ikk2 on its own expression level.

To determine whether the *ikk2* mutation inhibits NF-κB activation, we injected TLR5 agonist, flagellin, into the blood island of zebrafish embryos at 28 hpf and checked *il1b* expression at 1hpi as previously described (56). We found that *il1b* shows a significant upregulation in the *ikk2* mutant, and that the induction of the expression level was even much higher than in *ikk2*$^{+/+}$ larvae (Fig. 4E). This is a surprising result since the *ikk2*^{m10} mutation is predicted to lead to the absence of the whole Ikk2 protein and

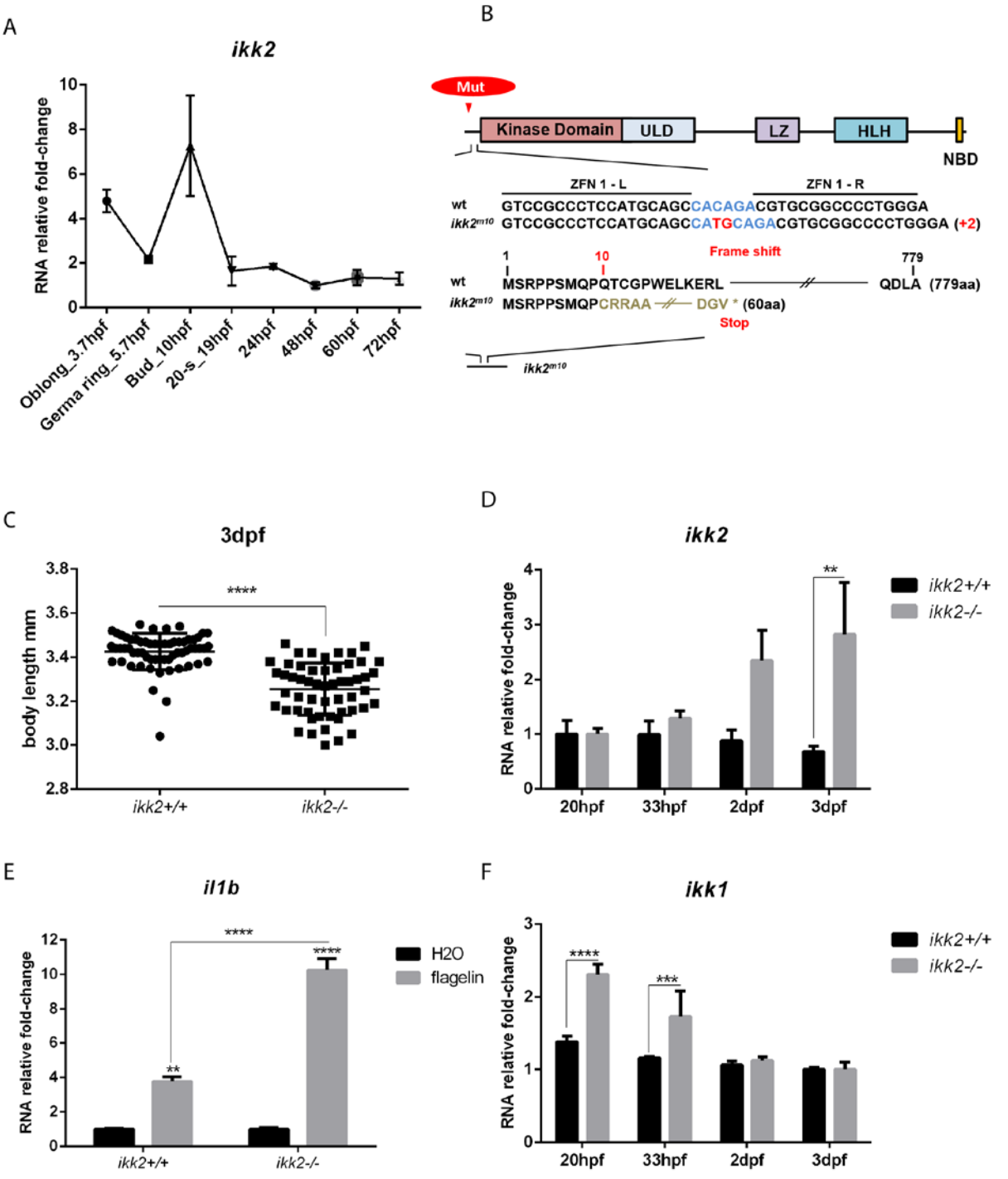

FIGURE 4 Characterization of *ikk2* and *ikk1* mRNA expression in the *ikk2*^{m10} mutant. A, mRNA expression analysis of *ikk2* from 3.7 to 72hpf in wildtype (AB/TL). B, *ikk2* mutant sequence and protein structure. An insertion mutation of two bases (AC to A**TG**C) in the N-terminal sequence of the kinase domain of zebrafish Ikk2 leads to a frame shift at the codon for the tenth amino acid and introduces a premature stop codon at the sixty first amino acid. The truncated protein lacks the whole Ikk2 protein. Nucleotide and amino acid positions are indicated with respect to the mutation position. C, larvae of *ikk2*$^{+/+}$ and *ikk2*$^{m10/m10}$ were imaged using stereo microscopy and their body length were measured at 3dpf. Statistical significance of differences was determined by *t*-test,

****p<0,0001. D, the mRNA expression of *ikk2* from 20hpf to 3dpf in *ikk2*$^{+/+}$ and *ikk2*$^{m10/m10}$ larvae. E, *il1b* mRNA expression in *ikk2*$^{+/+}$ and *ikk2*$^{m10/m10}$ embryos at 1hpi after flagellin blood island injection. F, the mRNA expression of *ikk1* from 20hpf to 3dpf in *ikk2*$^{+/+}$ and *ikk2*$^{m10/m10}$ larvae. Statistical significance of differences in D-F was determined by two-way ANOVA with Sidak Multiple Comparison test as a post-hoc test, ***p<0,001, ****p<0,0001.

should disrupt its function of phosphorylating IκB molecules, the inhibitors of NF-κB transcription factors. These disruptions will subsequently inhibit the release and nuclear translocation of NF-κB.

2 the Ikk2 mutation induces a temporary upregulation of Ikk1

Theoretically, phosphorylation of IKK2 is necessary for activation of the canonical NF-κB pathway (57) and IKK1, also known as IKKα or CHUK, is necessary for activation of the non-canonical or alternative pathway (58). Functioning as one of the catalytic subunits of the IKK complex, IKK1 shows a similar structure as IKK2 (59). A previous study in human lymphoma cells showed that IKKα may directly phosphorylate IκBα under conditions of IKKβ inhibition contributing to cell survival. Therefore, we studied the gene expression level of *ikk1* in *ikk2*$^{m10/m10}$ embryos and larvae. As the results show (Fig. 4F), the expression level of *ikk1* was significantly upregulated at 20 and 33hpf in *ikk2*$^{m10/m10}$ compared to *ikk2*$^{+/+}$ embryos, but after that it decreased to the normal level as shown in the *Ikk2*$^{+/+}$ larvae at 2 and 3dpf. These results suggest the hypothesis that *ikk2* deficiency may lead to *ikk1* overexpression in zebrafish embryos at an early stage, which induces a compensatory activation of the canonical NF-κB pathway.

3 The ikk2 mutant shows a deficient phenotype of leukocytes and is more susceptible to infection with Mycobacterium marinum than the wildtype

To characterize the phenotype of immune cells in *ikk2* mutant embryos, we performed a combination of TSA and L-plastin immunostaining in embryos at 2 and 3dpf (Fig. 5A, B). Cells labeled with TSA are neutrophils, and those labeled with L-plastin represent all leukocytes (i.e. neutrophils and macrophages). We found that there is a significant decrease in the number of neutrophils at 2dpf but not at 3 dpf (Fig. 5A, B). Furthermore, the total number of leukocytes seemed reduced at both 2 and 3 dpf, although not reaching the significance threshold (Fig. 5A, B). To confirm these result, we conducted qPCR to detect the transcript level of the genes *mpx* and *mpeg1* (Fig. 5C, D), which are marker genes of neutrophils and macrophages respectively. The expression level of these two genes showed a significant downregulation in the *ikk2*

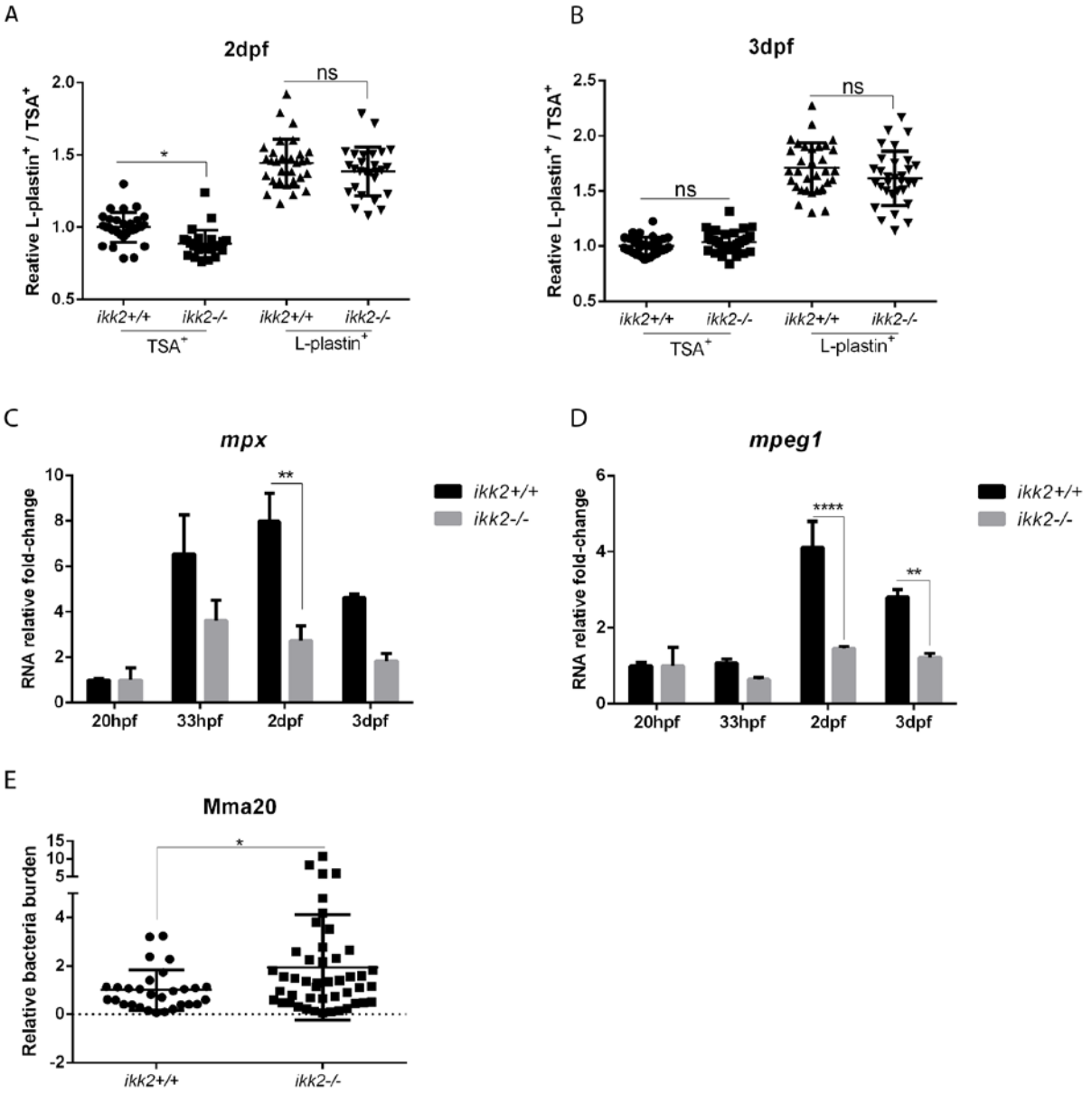

FIGURE 5 Study of leukocytes and mycobacterial infection in the Ikk2 mutant. A, B, quantification of leukocyte numbers. The number of neutrophils and macrophages was determined by performing whole mount L-plastin immuno-histochemistry (total leukocytes) combined with TSA staining (neutrophils) in 2 and 3dpf zebrafish larvae (n>=27). Statistical significance of differences was determined by *t*-test, *p < 0.05, **p<0,01. C, D, mRNA expression levels of *mpx* and *mpeg1* were determined by qPCR from 20hpf to 3dpf. E, quantification of bacterial burden. i*kk2*$^{+/+}$ and *ikk2*$^{-/-}$ embryos were infected at 28hpf with ~150CFU Mma20 strain. Stereo fluorescence images of Mm infected embryos at 4dpi were used for quantification of bacterial fluorescence pixels. Statistical significance of differences was determined by *t*-test, *p < 0.05.

mutant at 2 and 3dpf (Fig. 5C, D). Our results indicate therefore that in the *ikk2* mutant both neutrophil and macrophage development is affected.

Considering the deficiency of macrophages and neutrophils in the *ikk2* mutant at an early developmental stage, we performed an infection assay with *Mycobacterium marinum* m20 (Mma20) through blood island injection at 28hpf and detected the bacterial burden at 4dpi. The result shows that the *ikk2*$^{m10/m10}$ mutation promotes an increase of bacterial proliferation compared to the sibling control (Fig. 5E).

The effect of a mutation of Ikk2 on immune responses was also demonstrated in rodents. For instance, compared to the wildtype , mice with Ikk2 deficiency in lung epithelial cells exhibited a delayed onset of Th17 and B cell responses in the lung and delayed fungal clearance. Importantly, delayed Pneumocystis clearance in Ikk2-deficient mice was associated with an exacerbated immune response, impaired pulmonary function, and altered lung histology. These data demonstrate that Ikk2-dependent lung epithelial cell responses are important regulators of pulmonary adaptive immune responses and are required for optimal host defense against Pneumocystis infection (25).

4 The mutation of ikk2 modulates the insulin resistance induced by hyperinsulinemia

Mice with Ikk2 deficiency in myeloid cells retain global insulin sensitivity and are protected from insulin resistance (60). Zebrafish has been shown to be a good model to study acute insulin resistance induced by hyperinsulinemia in a previous study from our laboratory (61). To study how the *ikk2* zebrafish mutant responds to hyperinsulinemia, we injected insulin into the caudal aorta at 4dpf, and the second injection was conducted 240 minutes later following the protocol published previously. A glucose measurement was performed at 0, 30 and 240 minutes after the first injection and 30 minutes after the second injection. The results show a typical insulin resistance in wildtype larvae after the second injection, where they exhibited a significant higher glucose level (Fig. 6A). The result also show that there was no upregulation of the glucose level in *ikk2*$^{m10/m10}$ after the second insulin injection (Fig. 6C). We outcrossed the *ikk2*$^{m10/m10}$ mutant with the wildtype (AB/TL) leading to an offspring called *ikk2*$^{+/-}$. We found that in this heterozygote the glucose level increased after the second insulin injection as in the wildtype control (Fig. 6B).

To further study the role of IKK2 in insulin resistance, we measured the transcriptional level of the *phosphoenolpyruvate carboxykinase 1* gene (*pck1*), which is well known to be inhibited by insulin in mammals and zebrafish (62). As expected we found that the expression level of *pck1* in the wildtype was decreased after insulin injection (Fig. 6D). For the *ikk2*$^{+/-}$ with AB/TL background, analysis of *pck1* expression

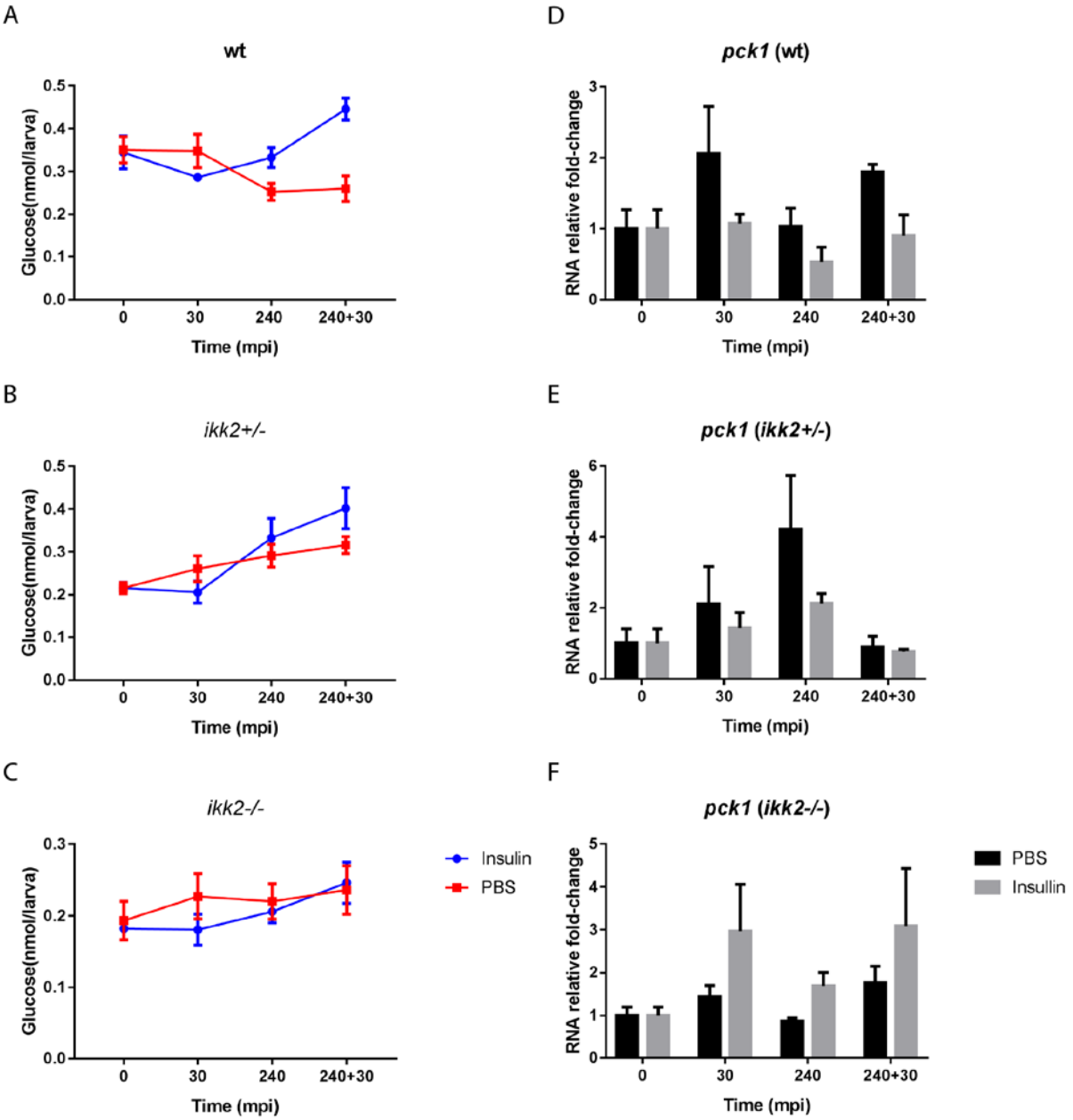

FIGURE 6 Studies of responses to hyperinsulinemia in the *ikk2* mutant. A-C, Zebrafish larvae from wildtype (A), *ikk2*$^{+/-}$ (B) and *ikk2*$^{-/-}$ (C) were injected with 1nl human recombinant insulin at 100 nM in the caudal aorta at 4 dpf and received a second injection at 4 hpi (240 min). Control larvae were injected with PBS. Samples for glucose measurements were taken at 0, 30, and 240 min after the first injection and 30 min after the second injection. Values in the scale are indicated in minutes post injection (mpi). Data (mean ± SE) are combined from 3 biological replicates (n= 4 or 5 larvae per group). D-F, mRNA expression level of *pck1* from wildtype (D), *ikk2*$^{+/-}$ (E) and *ikk2*$^{-/-}$ (F) were determined by qPCR at the same time points as the glucose measurements.

showed a similar result as in the wildtype (Fig. 6E). In contrast, for the *ikk2*$^{m10/m10}$, the expression level of *pck1* showed an increase after the insulin injection (Fig. 6F). These results indicate that the inhibition of *pck1* induced by insulin is reversed in the *ikk2* mutant.

Our zebrafish Ikk2 mutant has demonstrated its value for studying a role of IKK2 in responses to insulin. The mechanism underlying these results might be related to the degradation of S6K protein in the absence of IKK2 activation (63). This suggestion is based on a previous report of Um et al. (64) who reported that knockout of S6K protected mice from obesity-induced insulin resistance. However, the conclusion that Ikk2 deficiency reverses insulin resistance has also been challenged by the study of Rohl et al (65), who showed that Ikk2 expression in mice skeletal muscle is not essential for obesity-induced insulin resistance in mice (65). Considering these conflicting results, additional studies of the function of IKK2 in insulin resistance are necessary. We expect that our zebrafish mutant will be of great use for such studies.

General conclusions

TLR signaling is involved in a multitude of physiological and pathological processes. The derivative question is how TLR signaling can be involved in so many processes? Therefore the mediators in TLR signaling have become major research targets. In the last decade, construction of mutations in rodent models became a common strategy to study the function of important genes in TLR signaling. However, the global deficiency of most of them has been shown to lead to a lethal phenotype in mice, and therefore the zebrafish model becomes a prominent candidate for further studies because of its suitability for studies at the embryonic and larval stages. For example, in our study the *Ikk2* mutant was shown to be a potential model to study the mechanism of acute insulin resistance in the larval stage. This is based on our conclusion that in the *ikk2*$^{m10/m10}$ mutant the acute insulin resistance induced by hyperinsulinemia was modulated. Furthermore, the Ikk2 zebrafish mutant showed defects in development and immunity, such as decreased body length, lower leukocyte numbers, lower expression level of marker genes of immune cells and higher bacterial proliferation upon Mm infection. Unexpectedly, we found that the *ikk2* mutant induced an overexpression of *ikk1*, which may play a compensatory role in NF-κB activation and *il1b* expression. In future research, the Ikk2 deficiency model provides a chance to further study the interaction between the innate immune system and metabolic diseases.

In addition, we can also expect that an effective mutant of Traf6 can be generated in the near future, which not only can be applied in studies of immune-related diseases but also metabolic diseases, like diabetes, as well. This is expected because it has been

reported that blocking Cd40-Traf6 signaling is a therapeutic target in obesity-associated insulin resistance in mice (66).

Materials and methods

Zebrafish husbandry

The *traf6*^{sa244} mutant allele was identified by sequencing of an ENU-mutagenized zebrafish library. The mutant line was obtained from the Sanger Institute Zebrafish Mutation Resource. We performed an incross between the Fo generation of Traf6 heterozygotes, and only one male Traf6 homozygote offspring survived. Outcrosses of the heterozygote lines unfortunately did not survive and therefore we could only continue with the incrossed homozygote line. The *ikk2*^{m10} mutant allele was obtained from Dr. Vladimir Korzh from the Institute of Molecular and Cell Biology (Singapore). Heterozygous and homozygous carriers of the mutation were outcrossed twice with the wildtype (AB/TL strain), and were subsequently incrossed twice. Homozygous fish of the resulting family were used to produce embryos.

Wildtype zebrafish of the AB/TL strain and strains *traf6*$^{sa244/sa244}$, *traf6*$^{+/+}$, *traf6*$^{sa244/sa244}$/*Tg*(*mpeg1.1:mCherryF/mpx:GFP*), *traf6*$^{+/+}$/*Tg*(*mpeg1.1:mCherryF/mpx:GFP*), *ikk2*$^{m10/m10}$ and *ikk2*$^{+/+}$ strain were handled in compliance with the local animal welfare regulations and maintained according to standard protocols (zfin. org). Embryos and larvae were raised in egg water (60g/ml Instant Ocean sea salts) at 28.5 °C. For the duration of bacterial injections, larvae were kept under anesthesia in egg water containing 0.02% buffered 3-aminobenzoic acid ethyl ester (Tricaine, Sigma-Aldrich, the Netherlands). The culture of zebrafish carrying mutations that might cause immune deficiencies was approved by the local animal welfare committee (DEC) of the University of Leiden. All protocols adhered to the international guidelines specified by the EU Animal Protection Directive 2010/63/EU.

Bacterial strain preparation

The bacterial strains, *Mycobacterium marinum* (ATCC#BAA-535) m20 (Mma20) and E11 (MmE11), containing the plasmid pSMT3-mCherry (67), were used for the infection of zebrafish larvae. For the infection assay, bacteria were prepared as previously described (68), where the injection inoculum was prepared in 2% polyvinylpyrrolidone40 (PVP40) solution (CalBiochem), and 150 colony-forming units (CFU) of Mma20 were injected into the blood stream at 28 hours post fertilization (hpf) as previously described (68). For the yolk injection, 40 CFU of MmE11 were injected into the yolk around the 64 cell-stage as previously described (68).

Ligands injection

Purified Pam3CSK4 (InvivoGen, France) and flagellin from *S. typhimurium* (Flagellin FliC VacciGrade™, Invitrogen, France) were diluted in 1 mg/ml and 100 µg/ml in sterile water, respectively. For injection, 1 nl of the ligand solutions were injected into the blood stream at 28hpf. Sterile water was injected as a control experiment. Injections were performed using a FemtoJet microinjector (Eppendorf, the Netherlands) equipped with a capillary glass needle.

Insulin injection

To inject PBS and human recombinant insulin (Sigma–Aldrich, the Netherlands), 1nl was injected into the caudal aorta of 4 dpf zebrafish larvae using a glass capillary.

Glucose measurements

Glucose measurements were done using a fluorescence-based enzymatic detection kit (Biovision, Inc., Mountain View, CA, USA) as described previously (69).

Morpholino injections

Morpholino oligonucleotides (Gene Tools) were diluted to desired concentrations in 1× Danieu's buffer (58mM NaCl, 0.7mM KCl, 0.4mM $MgSO_4$, 0.6mM Ca $(NO_3)_2$, 5.0mM HEPES (pH 7.6)) containing 1× phenol red (Sigma-Aldrich). For knockdown experiments, *traf6* ATG-morpholino (*traf6* mo, 5'-GCCTATACTGCTGCTTCCTGTAA AG-3') was injected with the optimal concentration at 0.5 mM and 1nl volume per embryo at 0~2 cell stage. Control larvae were injected with the standard control morpholino (Sc mo, 5'- CCTCTTACCTCAGTTACAATTTATA-3').

Immunohistochemistry

Embryos or larvae were fixed in 4% paraformaldehyde in PBS overnight at 4°C. Mpx activity was detected with TSA (TSA plus kit, Fluorescence Systems, Perkin Elmer Inc., Waltham,MA) as previously described (70). Immunostaining with L-plastin antibody (71) and the secondary antibody was as described (72).

Infection assays and imaging

Zebrafish larvae were staged at 28 hours post fertilization (hpf) by morphological criteria (73), and ~150 CFU of Mma20 m-cherry strain were injected into the blood island under the dorsal aorta, sterile PBS injection using as negative control. Injections were controlled using a FemtoJet microinjector (Eppendorf) and a micromanipulator with pulled microcapillary pipettes. Pools of around 20 larvae were collected at 3- and 4-day post infection (dpi) and performed imaging on a Leica MZ16FA Fluorescence Stereo Microscope. Bright field and fluorescence images were generated with a Leica DC500 (DFC420C) camera. Bacterial loads were analyzed using dedicated pixel

counting software as previously described (74). Experiments were performed in triplicate.

COPAS analysis

Zebrafish larvae were injected with ~40 CFU of MmE11 m-cherry strain at 64 cell stage, and the bacteria burden was measured with COPAS at 3, 4 and 5dpf as previously described (75).

Western blot analysis

Western blot analysis were performed as previously described (61).Whole homogenized zebrafish 1dpf embryos (n=100/sample) or 4dpf larvae (n=15/sample) were prepared for protein isolation. The protein concentration was determined using a BCA Protein Assay Kit (Thermo Scientific, Rockford, IL, USA). The extracted protein samples were subjected to SDS–PAGE and transferred onto nitrocellulose membranes (Bio-Rad). The primary antibody is anti-TRAF6 (Abcam, EP591Y), and Pan-actin (Cell Signaling, no. 4968) was used as a loading control. Finally, the bands were quantified by densitometry using ImageJ Software (National Institutes of Health, Bethesda, MD, USA). The bands were quantified by densitometry using ImageJ 64 Software (National Institutes of Health).

Acknowledgments

We thank all members of the fish facility team for fish caretaking. We would like to thank to Saskia Rueb for preparing Jurkat cells. S. Y. was supported by a grant from the China Scholarship Council (CSC).

The zebrafish *traf6* mutant was obtained from the Sanger Institute Zebrafish Mutation Resource (ZF-MODELS Integrated Project funded by the European Commission; contract number LSHG-CT-2003-503496), also sponsored by the Welcome Trust [grant number WT 077047/Z/05/Z].

Supplementary data

Supplementary figure 1 Overview of the process of outcrosses and incrosses of the Traf6 mutant

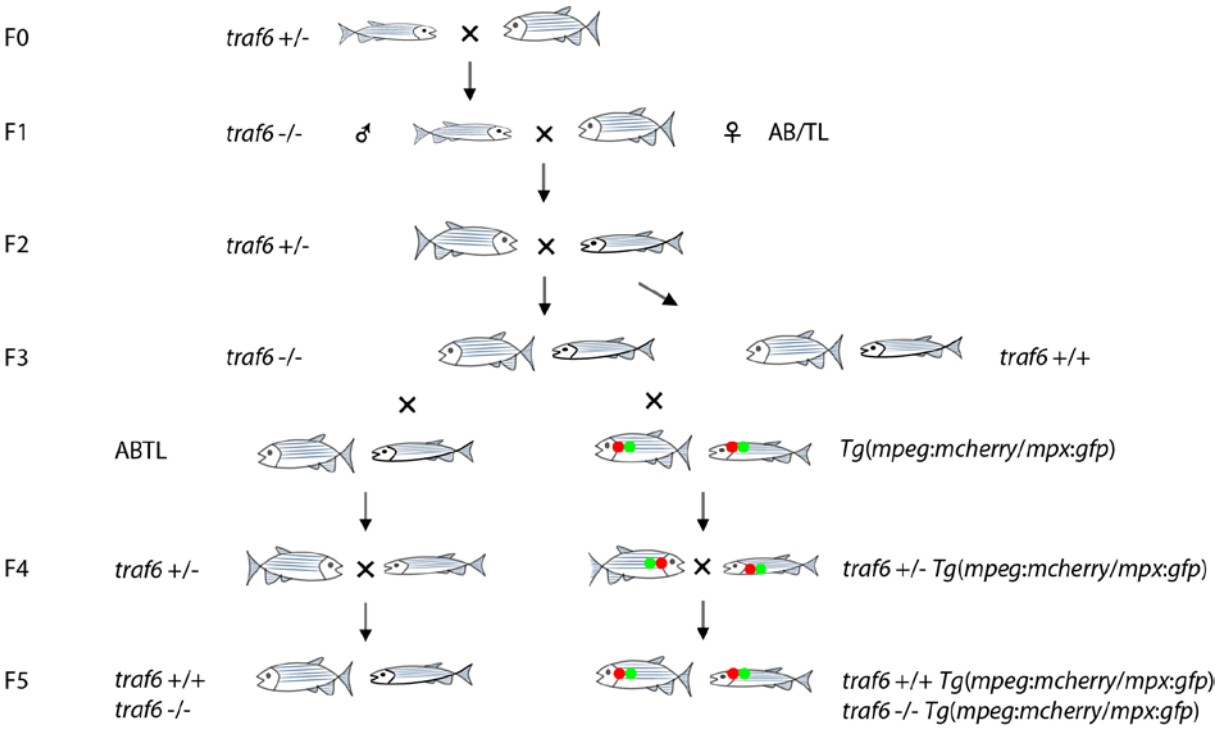

References

1. Akira, S., and K. Takeda. 2004. Toll-like receptor signalling. *Nat Rev Immunol* 4: 499-511.
2. Bradley, J. R., and J. S. Pober. 2001. Tumor necrosis factor receptor-associated factors (TRAFs). *Oncogene* 20: 6482-6491.
3. Sorrentino, A., N. Thakur, S. Grimsby, A. Marcusson, V. von Bulow, N. Schuster, S. Zhang, C. H. Heldin, and M. Landstrom. 2008. The type I TGF-beta receptor engages TRAF6 to activate TAK1 in a receptor kinase-independent manner. *Nat Cell Biol* 10: 1199-1207.
4. Yamashita, M., K. Fatyol, C. Jin, X. Wang, Z. Liu, and Y. E. Zhang. 2008. TRAF6 mediates Smad-independent activation of JNK and p38 by TGF-beta. *Mol Cell* 31: 918-924.
5. Ishida, T., S. Mizushima, S. Azuma, N. Kobayashi, T. Tojo, K. Suzuki, S. Aizawa, T. Watanabe, G. Mosialos, E. Kieff, T. Yamamoto, and J. Inoue. 1996. Identification of TRAF6, a novel tumor necrosis factor receptor-associated factor protein that mediates signaling from an amino-terminal domain of the CD40 cytoplasmic region. *J Biol Chem* 271: 28745-28748.
6. Walsh, M. C., J. Lee, and Y. Choi. 2015. Tumor necrosis factor receptor- associated factor 6 (TRAF6) regulation of development, function, and homeostasis of the immune system. *Immunol Rev* 266: 72-92.
7. Dickson, K. M., A. L. Bhakar, and P. A. Barker. 2004. TRAF6-dependent NF-kB transcriptional activity during mouse development. *Dev Dyn* 231: 122-127.
8. Naito, A., H. Yoshida, E. Nishioka, M. Satoh, S. Azuma, T. Yamamoto, S. Nishikawa, and J. Inoue. 2002. TRAF6-deficient mice display hypohidrotic ectodermal dysplasia. *Proc Natl Acad Sci U S A* 99: 8766-8771.
9. Lomaga, M. A., W.-C. Yeh, I. Sarosi, G. S. Duncan, C. Furlonger, A. Ho, S. Morony, C. Capparelli, G. Van, S. Kaufman, A. van der Heiden, A. Itie, A. Wakeham, W. Khoo, T. Sasaki, Z. Cao, J. M. Penninger, C. J. Paige, D. L. Lacey, C. R. Dunstan, W. J. Boyle, D. V. Goeddel, and T. W. Mak. 1999. TRAF6 deficiency results in osteopetrosis and defective interleukin-1, CD40, and LPS signaling. *Genes Dev* 13: 1015-1024.
10. Landstrom, M. 2010. The TAK1-TRAF6 signalling pathway. *Int J Biochem Cell Biol* 42: 585-589.
11. Yeiser, E. C., N. J. Rutkoski, A. Naito, J. Inoue, and B. D. Carter. 2004. Neurotrophin signaling through the p75 receptor is deficient in traf6-/- mice. *J Neurosci* 24: 10521-10529.
12. Inoue, J., J. Gohda, T. Akiyama, and K. Semba. 2007. NF-kappaB activation in development and progression of cancer. *Cancer Sci* 98: 268-274.
13. Liu, H., S. Tamashiro, S. Baritaki, M. Penichet, Y. Yu, H. Chen, J. Berenson, and B. Bonavida. 2012. TRAF6 activation in multiple myeloma: a potential therapeutic target. *Clin Lymphoma Myeloma Leuk* 12: 155-163.
14. Kobayashi, T., P. T. Walsh, M. C. Walsh, K. M. Speirs, E. Chiffoleau, C. G. King, W. W. Hancock, J. H. Caamano, C. A. Hunter, P. Scott, L. A. Turka, and Y. Choi. 2003. TRAF6 Is a Critical Factor for Dendritic Cell Maturation and Development. *Immunity* 19: 353-363.
15. Lomaga, M. A., J. T. Henderson, A. J. Elia, J. Robertson, R. S. Noyce, W. C. Yeh, and T. W. Mak. 2000. Tumor necrosis factor receptor-associated factor 6 (TRAF6) deficiency results in exencephaly and is required for apoptosis within the developing CNS. *J Neurosci* 20: 7384-7393.
16. Chiffoleau, E., T. Kobayashi, M. C. Walsh, C. G. King, P. T. Walsh, W. W. Hancock, Y. Choi, and L. A. Turka. 2003. TNF receptor-associated factor 6 deficiency during hemopoiesis induces Th2-polarized inflammatory disease. *J Immunol* 171: 5751-5759.
17. Muto, G., H. Kotani, T. Kondo, R. Morita, S. Tsuruta, T. Kobayashi, H. Luche, H. J. Fehling, M. Walsh, Y. Choi, and A. Yoshimura. 2013. TRAF6 is essential for maintenance of regulatory T cells that suppress Th2 type autoimmunity. *PLoS One* 8: e74639.
18. Gorjestani, S., B. G. Darnay, and X. Lin. 2012. Tumor necrosis factor receptor-associated factor 6 (TRAF6) and TGFbeta-activated kinase 1 (TAK1) play essential roles in the C-type lectin receptor signaling in response to Candida albicans infection. *J Biol Chem* 287: 44143-44150.
19. Mason, N. J., J. Fiore, T. Kobayashi, K. S. Masek, Y. Choi, and C. A. Hunter. 2004. TRAF6-dependent mitogen-activated protein kinase activation differentially regulates the production of interleukin-12 by macrophages in response to Toxoplasma gondii. *Infect Immun* 72: 5662-5667.
20. Li, Z. W., W. Chu, Y. Hu, M. Delhase, T. Deerinck, M. Ellisman, R. Johnson, and M. Karin. 1999. The IKKbeta subunit of IkappaB kinase (IKK) is essential for nuclear factor kappaB activation and prevention of apoptosis. *J Exp Med* 189: 1839-1845.
21. Tanaka, M., M. E. Fuentes, K. Yamaguchi, M. H. Durnin, S. A. Dalrymple, K. L. Hardy, and D. V. Goeddel. 1999. Embryonic lethality, liver degeneration, and impaired NF-kappa B activation in IKK-beta-deficient mice. *Immunity* 10: 421-429.
22. Lu, H., Q. Lu, S. Gaddipati, R. B. Kasetti, W. Wang, M. Pasparakis, H. J. Kaplan, and Q. Li. 2014. IKK2 inhibition attenuates laser-induced choroidal neovascularization. *PLoS One* 9: e87530.
23. Luedde, T., U. Assmus, T. Wustefeld, A. Meyer zu Vilsendorf, T. Roskams, M. Schmidt-Supprian, K. Rajewsky, D. A. Brenner, M. P. Manns, M. Pasparakis, and C. Trautwein. 2005. Deletion of IKK2 in hepatocytes does not sensitize these cells to TNF-induced apoptosis but protects from ischemia/reperfusion injury. *J Clin Invest* 115: 849-859.
24. Pasparakis, M., G. Courtois, M. Hafner, M. Schmidt-Supprian, A. Nenci, A. Toksoy, M. Krampert, M. Goebeler, R. Gillitzer, A. Israel, T. Krieg, K. Rajewsky, and I. Haase. 2002. TNF-mediated inflammatory skin disease in mice with epidermis-specific deletion of IKK2. *Nature* 417: 861-866.

25. Perez-Nazario, N., J. Rangel-Moreno, M. A. O'Reilly, M. Pasparakis, F. Gigliotti, and T. W. Wright. 2013. Selective ablation of lung epithelial IKK2 impairs pulmonary Th17 responses and delays the clearance of Pneumocystis. *J Immunol* 191: 4720-4730.
26. Caposio, P., T. Musso, A. Luganini, H. Inoue, M. Gariglio, S. Landolfo, and G. Gribaudo. 2007. Targeting the NF-kappaB pathway through pharmacological inhibition of IKK2 prevents human cytomegalovirus replication and virus-induced inflammatory response in infected endothelial cells. *Antiviral Res* 73: 175-184.
27. Heckmann, A., C. Waltzinger, P. Jolicoeur, M. Dreano, M. H. Kosco-Vilbois, and Y. Sagot. 2004. IKK2 inhibitor alleviates kidney and wasting diseases in a murine model of human AIDS. *Am J Pathol* 164: 1253-1262.
28. Amaya, M., K. Voss, G. Sampey, S. Senina, C. de la Fuente, C. Mueller, V. Calvert, K. Kehn-Hall, C. Carpenter, F. Kashanchi, C. Bailey, S. Mogelsvang, E. Petricoin, and A. Narayanan. 2014. The role of IKKbeta in Venezuelan equine encephalitis virus infection. *PLoS One* 9: e86745.
29. Yuan, M., N. Konstantopoulos, J. Lee, L. Hansen, Z. W. Li, M. Karin, and S. E. Shoelson. 2001. Reversal of obesity- and diet-induced insulin resistance with salicylates or targeted disruption of Ikkbeta. *Science* 293: 1673-1677.
30. Kim, J. K., Y. J. Kim, J. J. Fillmore, Y. Chen, I. Moore, J. Lee, M. Yuan, Z. W. Li, M. Karin, P. Perret, S. E. Shoelson, and G. I. Shulman. 2001. Prevention of fat-induced insulin resistance by salicylate. *J Clin Invest* 108: 437-446.
31. Wojciechowska, S., Z. Zeng, J. A. Lister, C. J. Ceol, and E. E. Patton. 2016. Melanoma Regression and Recurrence in Zebrafish. *Methods in molecular biology (Clifton, N.J.)* 1451: 143-153.
32. Tulotta, C., S. He, L. Chen, A. Groenewoud, W. van der Ent, A. H. Meijer, H. P. Spaink, and B. E. Snaar-Jagalska. 2016. Imaging of Human Cancer Cell Proliferation, Invasion, and Micrometastasis in a Zebrafish Xenogeneic Engraftment Model. *Methods in molecular biology (Clifton, N.J.)* 1451: 155-169.
33. Meijer, A. H. 2016. Protection and pathology in TB: learning from the zebrafish model. *Semin Immunopathol* 38: 261-273.
34. Myllymaki, H., C. A. Bauerlein, and M. Ramet. 2016. The Zebrafish Breathes New Life into the Study of Tuberculosis. *Front Immunol* 7: 196.
35. Saralahti, A., and M. Ramet. 2015. Zebrafish and Streptococcal Infections. *Scand J Immunol* 82: 174-183.
36. Stockhammer, O. W., A. Zakrzewska, Z. Hegedus, H. P. Spaink, and A. H. Meijer. 2009. Transcriptome profiling and functional analyses of the zebrafish embryonic innate immune response to Salmonella infection. *J Immunol* 182: 5641-5653.
37. Wager, K., A. A. Zdebik, S. Fu, J. D. Cooper, R. J. Harvey, and C. Russell. 2016. Neurodegeneration and Epilepsy in a Zebrafish Model of CLN3 Disease (Batten Disease). *PLoS One* 11: e0157365.
38. Martin-Jimenez, R., M. Campanella, and C. Russell. 2015. New zebrafish models of neurodegeneration. *Curr Neurol Neurosci Rep* 15: 33.
39. Brown, D. R., L. A. Samsa, L. Qian, and J. Liu. 2016. Advances in the Study of Heart Development and Disease Using Zebrafish. *J Cardiovasc Dev Dis* 3.
40. Kimmel, R. A., and D. Meyer. 2016. Zebrafish pancreas as a model for development and disease. *Methods Cell Biol* 134: 431-461.
41. Cao, Z., J. Xiong, M. Takeuchi, T. Kurama, and D. V. Goeddel. 1996. TRAF6 is a signal transducer for interleukin-1. *Nature* 383: 443-446.
42. Phelan, P. E., M. T. Mellon, and C. H. Kim. 2005. Functional characterization of full-length TLR3, IRAK-4, and TRAF6 in zebrafish (Danio rerio). *Mol Immunol* 42: 1057-1071.
43. Stockhammer, O. W., H. Rauwerda, F. R. Wittink, T. M. Breit, A. H. Meijer, and H. P. Spaink. 2010. Transcriptome analysis of Traf6 function in the innate immune response of zebrafish embryos. *Mol Immunol* 48: 179-190.
44. Naito, A., S. Azuma, S. Tanaka, T. Miyazaki, S. Takaki, K. Takatsu, K. Nakao, K. Nakamura, M. Katsuki, T. Yamamoto, and J. Inoue. 1999. Severe osteopetrosis, defective interleukin-1 signalling and lymph node organogenesis in TRAF6-deficient mice. *Genes Cells* 4: 353-362.
45. Kaji, K., R. Katogi, Y. Azuma, A. Naito, J. I. Inoue, and A. Kudo. 2001. Tumor necrosis factor alpha-induced osteoclastogenesis requires tumor necrosis factor receptor-associated factor 6. *J Bone Miner Res* 16: 1593-1599.
46. Lacey, D. C., A. Achuthan, A. J. Fleetwood, H. Dinh, J. Roiniotis, G. M. Scholz, M. W. Chang, S. K. Beckman, A. D. Cook, and J. A. Hamilton. 2012. Defining GM-CSF- and macrophage-CSF-dependent macrophage responses by in vitro models. *J Immunol* 188: 5752-5765.
47. Fleetwood, A. J., H. Dinh, A. D. Cook, P. J. Hertzog, and J. A. Hamilton. 2009. GM-CSF- and M-CSF-dependent macrophage phenotypes display differential dependence on type I interferon signaling. *J Leukoc Biol* 86: 411-421.
48. Hamilton, J. A. 2008. Colony-stimulating factors in inflammation and autoimmunity. *Nat Rev Immunol* 8: 533-544.
49. Stanley, E. R., K. L. Berg, D. B. Einstein, P. S. Lee, F. J. Pixley, Y. Wang, and Y. G. Yeung. 1997. Biology and action of colony--stimulating factor-1. *Mol Reprod Dev* 46: 4-10.
50. Wang, Y., C. Zhou, J. Huo, Y. Ni, P. Zhang, C. Lu, B. Jing, F. Xiao, W. Chen, W. Li, P. Zhang, and L. Zhang. 2015. TRAF6 is required for the GM-CSF-induced JNK, p38 and Akt activation. *Mol Immunol* 65: 224-229.
51. Zhang, L., Y. Wang, F. Xiao, S. Wang, G. Xing, Y. Li, X. Yin, K. Lu, R. Wei, J. Fan, Y. Chen, T. Li, P. Xie, L. Yuan, L. Song, L. Ma, L. Ding, F. He, and L. Zhang. 2014. CKIP-1 regulates macrophage proliferation by inhibiting TRAF6-mediated Akt activation. *Cell Res* 24: 742-761.
52. Li, Q., D. Van Antwerp, F. Mercurio, K. F. Lee, and I. M. Verma. 1999. Severe liver degeneration in mice lacking the IkappaB kinase 2 gene. *Science* 284: 321-325.

53. Hwang, W. Y., Y. Fu, D. Reyon, M. L. Maeder, S. Q. Tsai, J. D. Sander, R. T. Peterson, J. R. J. Yeh, and J. K. Joung. 2013. Efficient genome editing in zebrafish using a CRISPR-Cas system. *Nat Biotech* 31: 227-229.
54. Varshney, G. K., W. Pei, M. C. LaFave, J. Idol, L. Xu, V. Gallardo, B. Carrington, K. Bishop, M. Jones, M. Li, U. Harper, S. C. Huang, A. Prakash, W. Chen, R. Sood, J. Ledin, and S. M. Burgess. 2015. High-throughput gene targeting and phenotyping in zebrafish using CRISPR/Cas9. *Genome research* 25: 1030-1042.
55. Ashida, N., S. SenBanerjee, S. Kodama, S. Y. Foo, M. Coggins, J. A. Spencer, P. Zamiri, D. Shen, L. Li, T. Sciuto, A. Dvorak, R. E. Gerszten, C. P. Lin, M. Karin, and A. Rosenzweig. 2011. IKK[beta] regulates essential functions of the vascular endothelium through kinase-dependent and -independent pathways. *Nat Commun* 2: 318.
56. Yang, S., R. Marin-Juez, A. H. Meijer, and H. P. Spaink. 2015. Common and specific downstream signaling targets controlled by Tlr2 and Tlr5 innate immune signaling in zebrafish. *BMC Genomics* 16: 547.
57. Israël, A. 2010. The IKK Complex, a Central Regulator of NF-κB Activation. *Cold Spring Harbor Perspectives in Biology* 2: a000158.
58. Senftleben, U., Y. Cao, G. Xiao, F. R. Greten, G. Krahn, G. Bonizzi, Y. Chen, Y. Hu, A. Fong, S. C. Sun, and M. Karin. 2001. Activation by IKKalpha of a second, evolutionary conserved, NF-kappa B signaling pathway. *Science* 293: 1495-1499.
59. Lam, L. T., R. E. Davis, V. N. Ngo, G. Lenz, G. Wright, W. Xu, H. Zhao, X. Yu, L. Dang, and L. M. Staudt. 2008. Compensatory IKKα activation of classical NF-κB signaling during IKKβ inhibition identified by an RNA interference sensitization screen. *Proceedings of the National Academy of Sciences* 105: 20798-20803.
60. Arkan, M. C., A. L. Hevener, F. R. Greten, S. Maeda, Z. W. Li, J. M. Long, A. Wynshaw-Boris, G. Poli, J. Olefsky, and M. Karin. 2005. IKK-beta links inflammation to obesity-induced insulin resistance. *Nat Med* 11: 191-198.
61. Marin-Juez, R., S. Jong-Raadsen, S. Yang, and H. P. Spaink. 2014. Hyperinsulinemia induces insulin resistance and immune suppression via Ptpn6/Shp1 in zebrafish. *The Journal of endocrinology*.
62. O'Brien, R. M., and D. K. Granner. 1990. PEPCK Gene as Model of Inhibitory Effects of Insulin on Gene Transcription. *Diabetes Care* 13: 327-339.
63. Zhang, J., Z. Gao, and J. Ye. 2013. Phosphorylation and degradation of S6K1 (p70S6K1) in response to persistent JNK1 Activation. *Biochim Biophys Acta* 1832: 1980-1988.
64. Um, S. H., F. Frigerio, M. Watanabe, F. Picard, M. Joaquin, M. Sticker, S. Fumagalli, P. R. Allegrini, S. C. Kozma, J. Auwerx, and G. Thomas. 2004. Absence of S6K1 protects against age- and diet-induced obesity while enhancing insulin sensitivity. *Nature* 431: 200-205.
65. Rohl, M., M. Pasparakis, S. Baudler, J. Baumgartl, D. Gautam, M. Huth, R. De Lorenzi, W. Krone, K. Rajewsky, and J. C. Bruning. 2004. Conditional disruption of IkappaB kinase 2 fails to prevent obesity-induced insulin resistance. *J Clin Invest* 113: 474-481.
66. Chatzigeorgiou, A., T. Seijkens, B. Zarzycka, D. Engel, M. Poggi, S. van den Berg, S. van den Berg, O. Soehnlein, H. Winkels, L. Beckers, D. Lievens, A. Driessen, P. Kusters, E. Biessen, R. Garcia-Martin, A. Klotzsche-von Ameln, M. Gijbels, R. Noelle, L. Boon, T. Hackeng, K. M. Schulte, A. Xu, G. Vriend, S. Nabuurs, K. J. Chung, K. Willems van Dijk, P. C. Rensen, N. Gerdes, M. de Winther, N. L. Block, A. V. Schally, C. Weber, S. R. Bornstein, G. Nicolaes, T. Chavakis, and E. Lutgens. 2014. Blocking CD40-TRAF6 signaling is a therapeutic target in obesity-associated insulin resistance. *Proc Natl Acad Sci U S A* 111: 2686-2691.
67. van der Sar, A. M., H. P. Spaink, A. Zakrzewska, W. Bitter, and A. H. Meijer. 2009. Specificity of the zebrafish host transcriptome response to acute and chronic mycobacterial infection and the role of innate and adaptive immune components. *Mol Immunol* 46: 2317-2332.
68. Benard, E. L., A. M. van der Sar, F. Ellett, G. J. Lieschke, H. P. Spaink, and A. H. Meijer. 2012. Infection of zebrafish embryos with intracellular bacterial pathogens. *Journal of visualized experiments : JoVE*: 2.
69. Jurczyk, A., N. Roy, R. Bajwa, P. Gut, K. Lipson, C. Yang, L. Covassin, W. J. Racki, A. A. Rossini, N. Phillips, D. Y. R. Stainier, D. L. Greiner, M. A. Brehm, R. Bortell, and P. diIorio. 2011. Dynamic glucoregulation and mammalian-like responses to metabolic and developmental disruption in zebrafish. *General and Comparative Endocrinology* 170: 334-345.
70. Loynes, C. A., J. S. Martin, A. Robertson, D. M. Trushell, P. W. Ingham, M. K. Whyte, and S. A. Renshaw. 2010. Pivotal Advance: Pharmacological manipulation of inflammation resolution during spontaneously resolving tissue neutrophilia in the zebrafish. *J Leukoc Biol* 87: 203-212.
71. Mathias, J. R., M. E. Dodd, K. B. Walters, S. K. Yoo, E. A. Ranheim, and A. Huttenlocher. 2009. Characterization of zebrafish larval inflammatory macrophages. *Dev Comp Immunol* 33: 1212-1217.
72. Cui, C., E. L. Benard, Z. Kanwal, O. W. Stockhammer, M. van der Vaart, A. Zakrzewska, H. P. Spaink, and A. H. Meijer. 2011. Infectious disease modeling and innate immune function in zebrafish embryos. *Methods Cell Biol* 105: 273-308.
73. Kimmel, C. B., W. W. Ballard, S. R. Kimmel, B. Ullmann, and T. F. Schilling. 1995. Stages of embryonic development of the zebrafish. *Dev Dyn* 203: 253-310.
74. Stoop, E. J. M., T. Schipper, S. K. Rosendahl Huber, A. E. Nezhinsky, F. J. Verbeek, S. S. Gurcha, G. S. Besra, C. M. J. E. Vandenbroucke-Grauls, W. Bitter, and A. M. van der Sar. 2011. Zebrafish embryo screen for mycobacterial genes involved in the initiation of granuloma formation reveals a newly identified ESX-1 component. *Dis Model Mech* 4: 526-536.

75. Veneman, W. J., O. W. Stockhammer, L. de Boer, S. A. Zaat, A. H. Meijer, and H. P. Spaink. 2013. A zebrafish high throughput screening system used for Staphylococcus epidermidis infection marker discovery. *BMC Genomics* 14: 255.

4